SUPPLEMENTARY

In Vitro Isolation of Small-Molecule-Binding Aptamers with Intrinsic Dye-Displacement Functionality

Haixiang Yu[1], Weijuan Yang[1], Obtin Alkhamis[1], Juan Canoura[1], Kyung-Ae Yang[2] and Yi Xiao[1,*]

[1]Department of Chemistry and Biochemistry, Florida International University, 11200 SW Eighth Street, Miami, Florida 33199, United States
[2]Division of Experimental Therapeutics, Department of Medicine, Columbia University, New York, New York 10032, United States

DETAILED METHODS

Characterization of target displacement of Cy7 from TWJ-structured aptamers. 5 μL of DISS.1 aptamer or DOGS.1 aptamer (1) (final concentration: 7 μM), 5 μL of Cy7 (final concentration: 3 μM), 5 μL of DIS or DOG (final concentration: 0 or 250 μM), and 35 μL selection buffer (1) (20 mM Tris-HCl, 10 mM $MgCl_2$, 1 M NaCl, 0.01% Tween 20, 1% DMSO, pH 7.4) were mixed in wells of a 384-well plate. UV-vis spectra were immediately recorded from 450–900 nm using a Tecan Infinite M1000 PRO at room temperature.

Characterization of binding of Cy7 to TWJ pool. 5 μL of different concentrations of TWJ pool, 5 μL of 20 μM Cy7, and 40 μL of reaction buffer (final concentration 10 mM Tris-HCl, 0.5 mM $MgCl_2$, 20 mM NaCl, 0.01% Tween 20, and 1% DMSO, pH 7.4) were mixed in wells of a 384-well plate. UV-vis spectra were immediately recorded from 450 nm to 900 nm at room temperature. The absorbance value at 760 nm was plotted against the concentration of added TWJ pool. The K_D was estimated by non-linear fitting using the Langmuir equation.

Continuous variation experiment (Job plot). 10 μM Cy7 and 10 μM TWJ pool were separately prepared in reaction buffer. Different ratios of Cy7 and TWJ pool were then mixed, with the concentration of both species totaling 10 μM. 50 μL of each mixture was loaded into a 384-well plate, and UV-vis spectra were immediately recorded from 450–900 nm at room temperature. The absorbance at 760 nm was plotted versus the mole fraction of Cy7.

Development of a target elution assay to assess pool affinity and target specificity. After each round of SELEX, 50 pmole of the enriched pool was mixed with 250 pmole of biotinylated complementary strand (**Table S1,** cDNA-bio) in 125 μL binding buffer (10 mM Tris-HCl, 0.5 mM $MgCl_2$, 20 mM NaCl, 0.01% Tween 20%, pH 7.4). The mixture was heated to 95 °C for 5 min, slowly cooled down to room temperature over 30 min, and loaded into a micro-gravity column containing 125 μL of streptavidin-coated agarose resin for library immobilization. The library-immobilized resin was collected into a microcentrifugation tube and washed five times with 625 μL binding buffer on an end-to-end rotator to

remove unconjugated library and complementary stands. After washing, the library-conjugated resin was re-suspended in 150 μL binding buffer and aliquoted into six PCR tubes (20 μL each). 50 μL binding buffer containing different amounts of MDPV was added to these tubes to reach final target concentrations of 0, 10, 50, 100, 250, and 500 μM. After a 60-min incubation on an end-over-end rotator, the agarose resin was precipitated by centrifugation. 3 μL of supernatant was collected and mixed with 6 μL of gel loading buffer (75% formamide, 10% glycerol, 0.125% SDS, 10 mM EDTA, and 0.15% (w/v) xylene cyanol). 5 μL of each collected sample was then loaded into the wells of a 15% denaturing polyacrylamide gel. A control sample (40 nM initial random library) was also loaded into the gel to evaluate the concentration of target-eluted library in each sample. Separation was carried out at 20 V/cm for 1 hour in 0.5× TBE running buffer. The gel was stained with 1× SYBR Gold solution for 25 min and imaged using a ChemiDoc MP Image System (Bio-Rad). The percentages of elution were calculated from the concentration of target-eluted library and the initial amount of library used in immobilization, which were then plotted versus the concentration of MDPV. K_D of the library pool was estimated with non-linear curve fitting using the Langmuir equation. The target specificity for the enriched pool was tested using the method described above, by eluting library-immobilized agarose resin with binding buffer, 500 μM MDPV, 500 μM methamphetamine, 500 μM amphetamine and 500 μM dopamine.

Isothermal titration calorimetry (ITC) experiments. All ITC experiments were performed at 23 °C in reaction buffer with a MicroCal iTC200 instrument (Malvern). The sample cell contained 20 μM MA, 20 μM MA-L, 20 μM Cy7-MA complex (1:1), 20 μM Cy7:MA-L complex (1:1), or 20 μM cDNA:MA-L complex (1:1). The syringe contained 1 mM MDPV in reaction buffer. Each experiment consisted of 19 successive 2 μL injections after a 0.4 μL purge injection with spacing of 180 seconds to a final molar ratio of 11:1 (MDPV:aptamer). The raw data were first corrected based on the heat of dilution of target, and then analyzed with the MicroCal analysis kit integrated into Origin 7 software with a single-site binding model.

Strand-displacement fluorescence assay for detection of MDPV. First, the molar ratio between the fluorophore-labeled aptamer strand (**Table S1,** MA-F) and the quencher-labeled complementary strand (**Table S1**, cDNA-Q) was optimized. Specifically, 8 μL of MA-F (final concentration 50 nM) and 8 μL of different concentrations of cDNA-Q were mixed with reaction buffer to a total volume of 80 μL. The samples were then heated at 95 °C for 5 min and slowly cooled down to room temperature over 30 min. 75 μL of samples were loaded into a 384-well plate, and the fluorescence spectra were recorded from 655–850 nm with excitation at 648 nm at room temperature. To perform the strand-displacement fluorescence assay, reaction buffer containing 50 nM MA-F and 50 nM cDNA-Q (final concentration) was heated at 95 °C for 5 min and slowly cooled down to room temperature over 30 min. 8 μL of different concentrations of MDPV were then mixed with 72 μL of the cDNA-Q:MA-F complex in the wells of a 384-well plate. After 10 min of incubation, fluorescence spectra were recorded from 655–850 nm with excitation at 648 nm at room temperature. The signal gain was calculated by $(F-F_0)/F_0$, where F_0 and F are the fluorescence intensity at 668 nm without and with MDPV, respectively.

REFERENCES

1. Yang,K.A., Pei,R.J., Stefanovic,D. and Stojanovic,M.N. (2012) Optimizing cross-reactivity with evolutionary search for sensors. *J. Am. Chem. Soc.*, **134**, 1642–1647.

SUPPORTING TABLE AND FIGURES

Table S1: The sequences of DNA oligonucleotides employed in this work.

Sequence ID	Sequence (5' – 3')
DISS.1	CTCGGGACGTGGATTTTCCGCATACGAAGTTGTCCCGAG
DOGS.1	TCGGGACGTGGATTTTCCACAAACCAGAATGGTGTCCCGA
TWJ pool	CTTACGACNNNGGCATTTTGCCNNNNAACGAAGTTNNNGTCGTAAG
Library	CGAGCATAGGCAGAACTTACGACNNNGGNATTTTNCCNNNNANCGAAGNTNNNGTCGTAAGAGCGAGTCATTC
S1 stem-loop	CTTACGACTTTGTCGTAAG
S2 stem-loop	GGCATTTTGCC
S3 stem-loop	AACGAAGTT
cDNA-bio	TTTTTGTCGTAAGTTCTGCCATTTT/Bio/
FP	GCAGCATAGGCAGAACTTAC
RP	GAATGACTCGCTCTTACGAC
RP-bio	/Bio/GAATGACTCGCTCTTACGAC
MA	CTTACGACTCAGGCATTTTGCCGGGTAACGAAGTTACTGTCGTAAG
MA-L	CAGAACTTACGACTCAGGCATTTTGCCGGGTAACGAAGTTACTGTCGTAAG
MA-F	/5Cy5/GGCAGAACTTACGACTCAGGCATTTTGCCGGGTAACGAAGTTACTGTCGTAAG
cDNA	GTCGTAAGTTCTGCC
cDNA-Q	GTCGTAAGTTCTGCC/3IAbRQsp/

a. N represents random base

b. /Bio/ represents biotin modification

c. /5Cy5/ represents Cy5 fluorophore modification

/3IAbRQsp/ represents Iowa Black RQ quencher modification

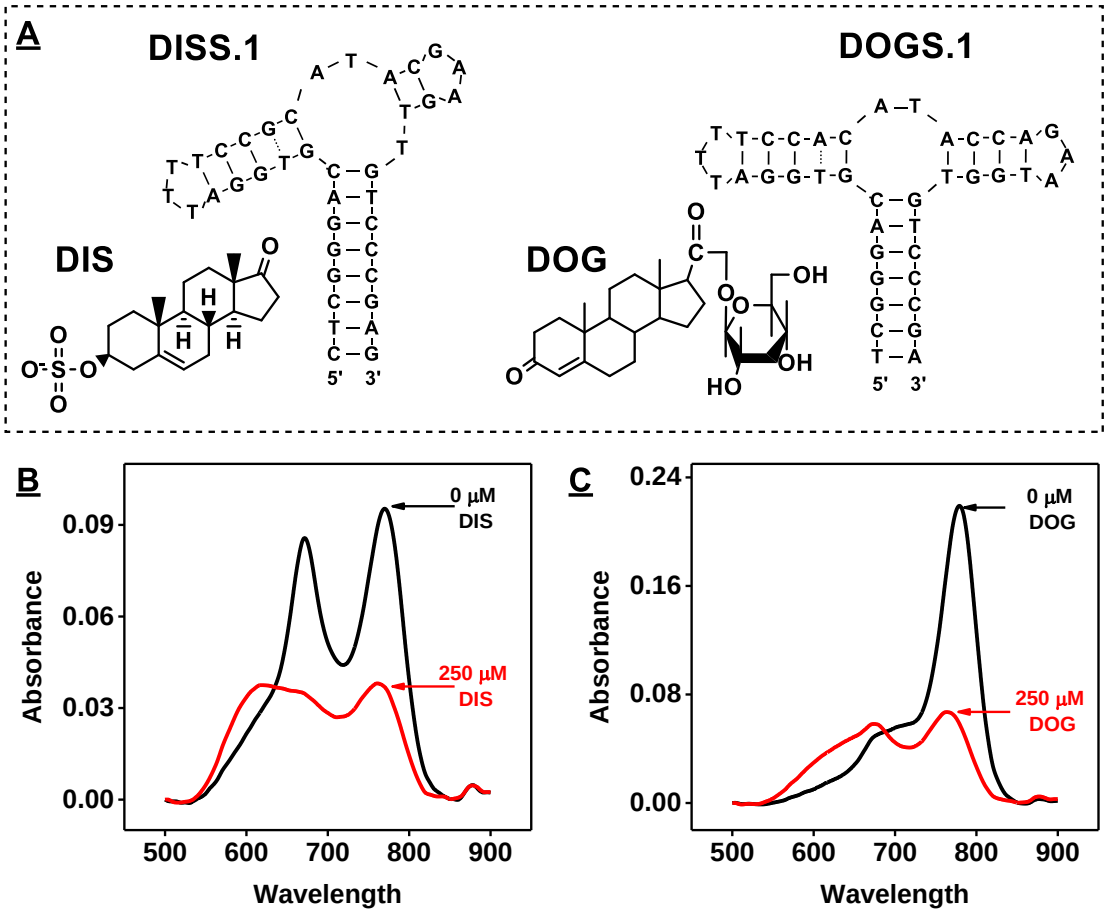

Figure S1. Generality of target-induced displacement of Cy7 from aptamers with a TWJ-structured binding domain. (**A**) Structure of dehydroisoandrosterone-3-sulfate (DIS) and deoxycorticosterone-21 glucoside (DOG) and their respective aptamers, DISS.1 and DOGS.1. Both aptamers contain a TWJ-structured binding domain. Absorbance spectra for a mixture of 3 µM Cy7 and 7 µM (**B**) DISS.1 or (**C**) DOGS.1 in the absence (black line) or presence (red line) of 250 µM DIS or DOGS, respectively. The greatly reduced Cy7 absorbance at 760 nm indicates successful displacement of Cy7 from the aptamer TWJ domain.

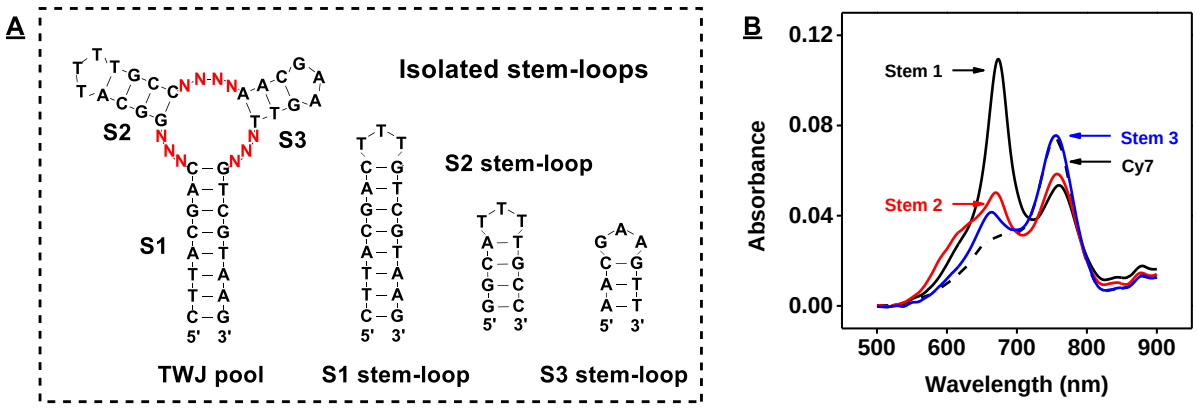

Figure S2. Characterization of Cy7 binding to the isolated stems from the TWJ pool. (**A**) Sequences of the TWJ pool and isolated S1, S2, and S3 stem-loops. (**B**) Binding of Cy7 to each isolated stem-loop. When 2 μM Cy7 was combined with 10 μM S1 stem-loop, only the absorbance of the dimer (670 nm) increased. Combination with either 10 μM S2 stem-loop or S3 stem-loop did not significantly enhance the absorbance of either the monomer or the dimer. The dashed line represents the spectrum of Cy7 alone.

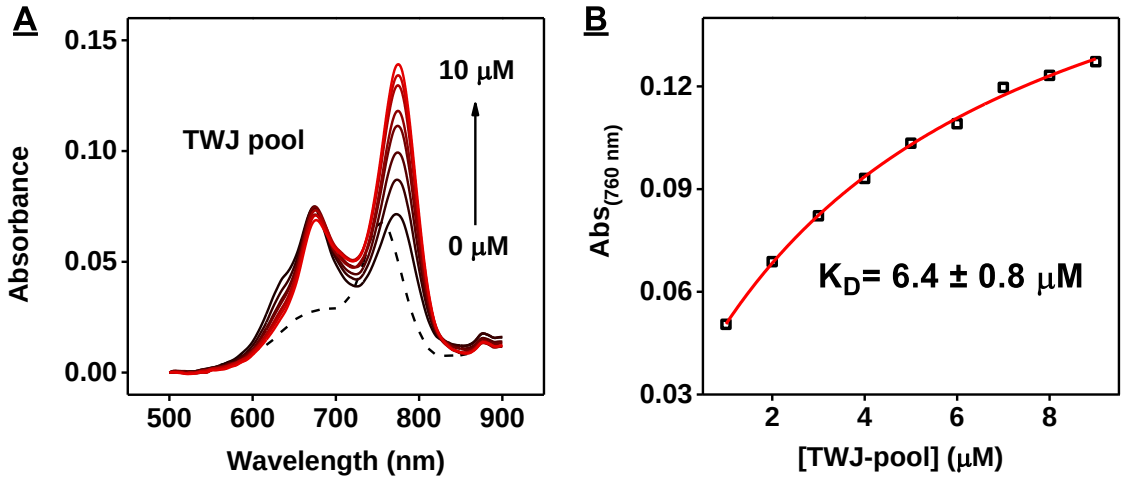

Figure S3. Characterization of Cy7 binding to the TWJ pool. (**A**) Titration of increasing amounts of the TWJ pool (2–10 μM) into 2 μM Cy7 resulted in enhanced absorbance of Cy7 at 760 nm, indicating interaction between the TWJ pool and the Cy7 monomer. The dashed line represents the spectrum of Cy7 alone. (**B**) Cy7 binding affinity for the TWJ pool was estimated from absorbance at 760 nm in the absence and presence of different concentrations of TWJ pool.

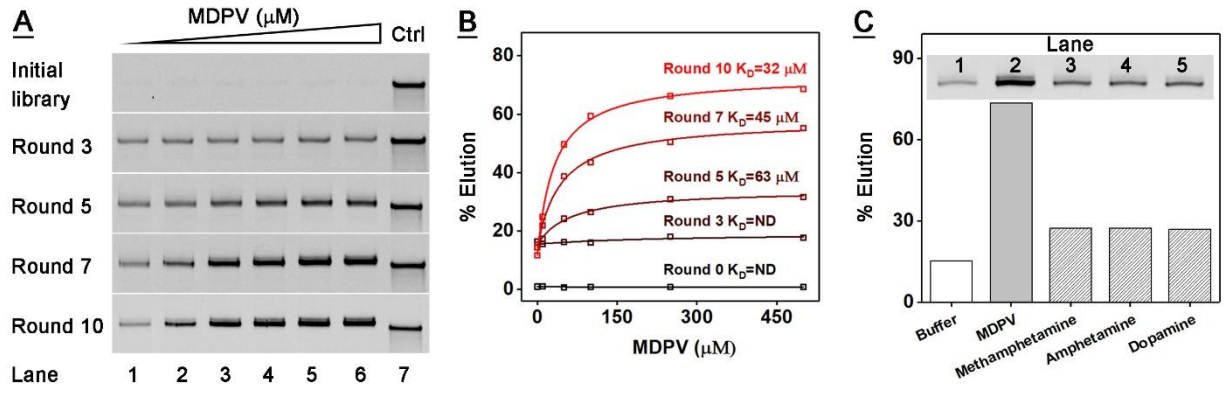

Figure S4. Estimation of target affinity and specificity of the enriched pools during SELEX using a target elution assay. (**A**) Target elution profile of the initial library and enriched pools after selection rounds 3, 5, 7, and 10 was analyzed by PAGE. Lanes 1-6 represent samples of the initial library and enriched pools eluted with 0, 10, 50, 100, 250, and 500 μM MDPV. Control samples (lane 7) containing 40 nM synthesized library were used to measure the concentration of eluted strands and percent elution of each sample. (**B**) The MDPV binding affinity of the library and enriched pools were calculated based on the percent elution of each sample. (**C**) The target specificity of the enriched pool after 10 rounds of SELEX was also assessed by the target elution assay. Inset shows the enriched pool eluted with binding buffer (lane 1), 500 μM MDPV (lane 2), 500 μM methamphetamine (lane 3), 500 μM amphetamine (lane 4), and 500 μM dopamine (lane 5).

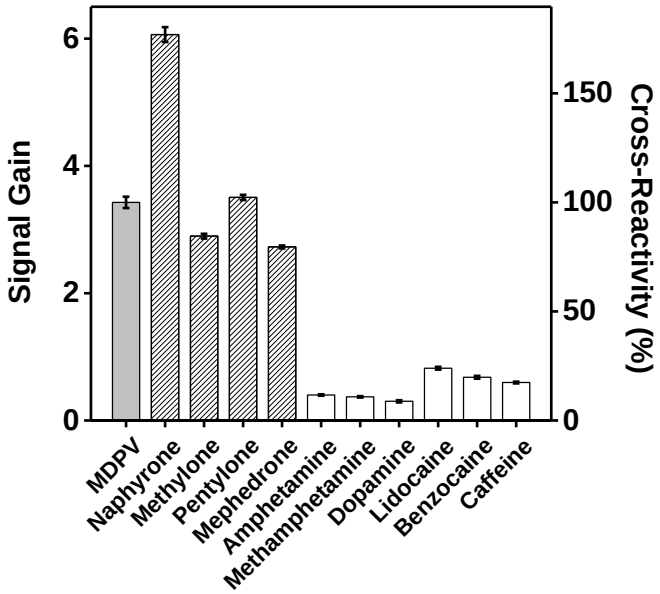

Figure S5. Cross-reactivity and specificity of our Cy7-displacement assay with 250 μM MDPV, other synthetic cathinones, or structurally-similar non-cathinone compounds and common cutting agents. Signal gain was calculated by $(R–R_0)/R_0$, where R and R_0 are the absorbance ratio at 670/760 nm with and without target/interfering agent, respectively. Error bars show standard deviation from three measurements of each compound tested.

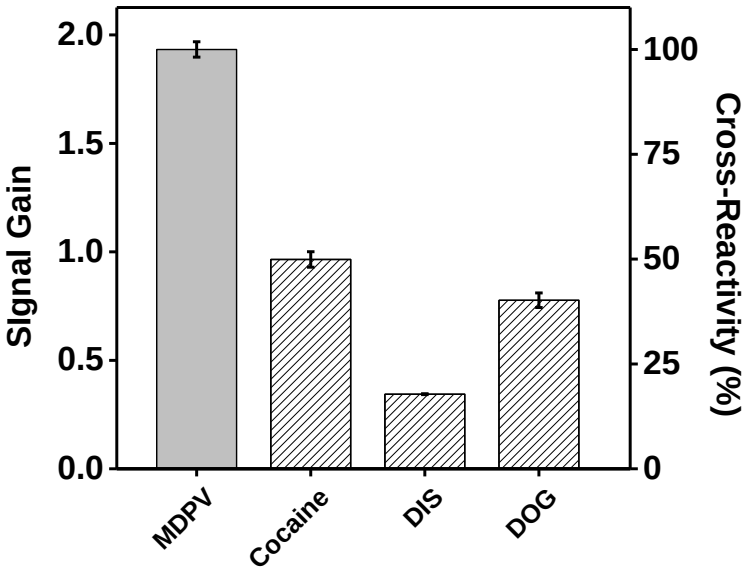

Figure S6. Cross-reactivity of our Cy7-displacement assay with 50 μM MDPV, cocaine, DIS and DOG. Error bars show standard deviation from three measurements of each compound.

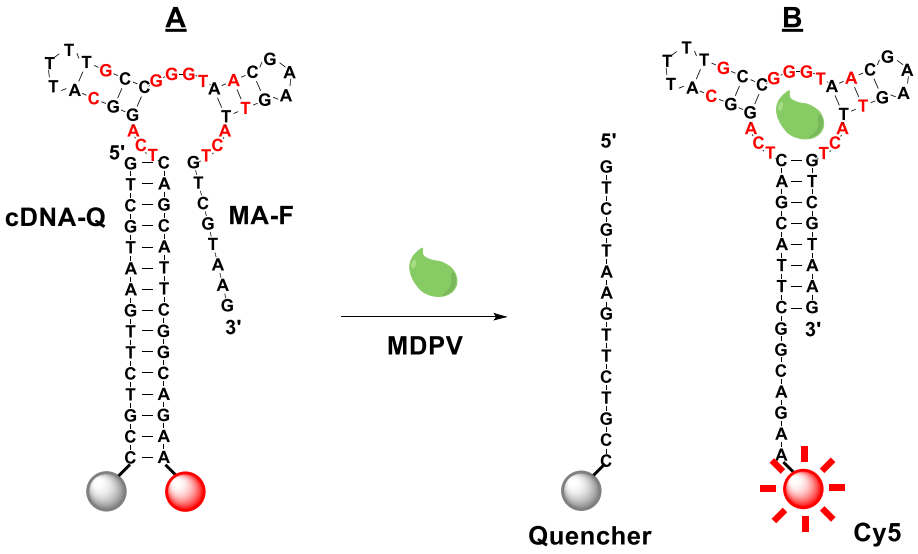

Figure S7. Working principle of a conventional strand-displacement fluorescence assay. (**A**) In the absence of MDPV, MA-F forms a 15-bp duplex with cDNA-Q, which situates the fluorophore in close proximity to the quencher, thus quenching fluorescence. (**B**) MDPV induces a target-induced conformational change in MA-F, forming a TWJ structure that results in dissociation of cDNA-Q, generating a measurable fluorescence signal.

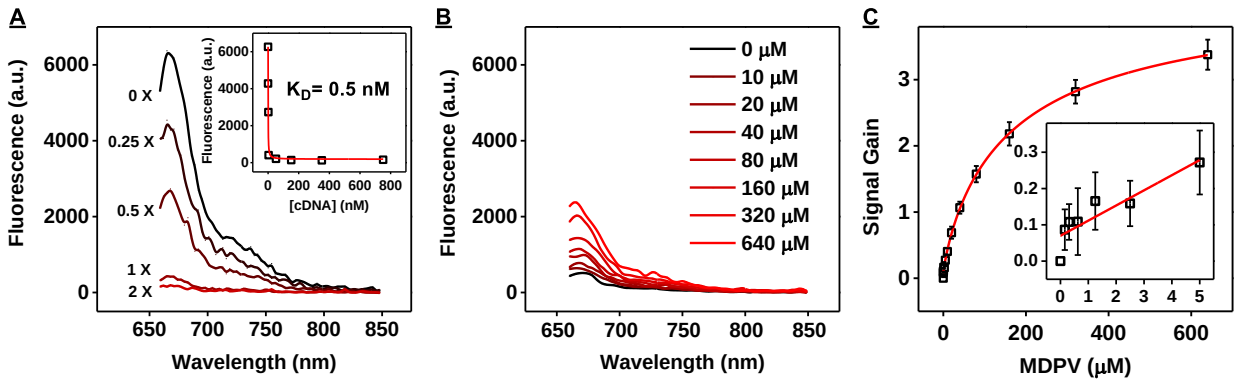

Figure S8. Strand-displacement fluorescence assay based on the MA aptamer. (**A**) Fluorescence spectra obtained from titration of cDNA-Q into a solution of MA-F at different molar ratios (0–2×). Inset shows binding affinity of cDNA-Q to MA-F as estimated from the fluorescence intensity at 668 nm in the absence and presence of different concentrations of cDNA-Q. (**B**) Fluorescence spectra obtained from titration of different concentrations of MDPV into 50 nM MA-F and 50 nM cDNA-Q. (**C**) Calibration curves for the strand-displacement fluorescence assay. Inset shows assay performance at a low concentration range. Error bars show standard deviation from three measurements at each concentration.

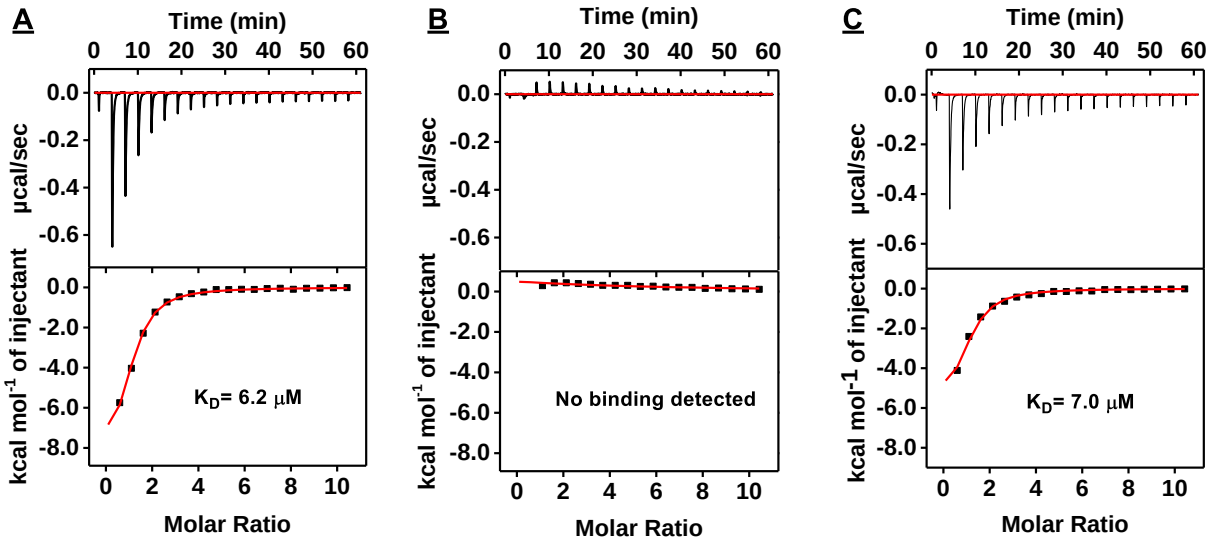

Figure S9. ITC characterization of MDPV binding affinity to (**A**) MA-L alone, (**B**) cDNA-MA-L complex (1:1), and (**C**) Cy7-MA-L complex (1:1). The top panels display raw data showing the heat generated from each titration of MDPV. The bottom panels show the integrated heat of each titration after correcting for dilution heat of the titrant.